

Doping-Dependent Photon Scattering Resonance in the Model High-Temperature Superconductor $\text{HgBa}_2\text{CuO}_{4+\delta}$ Revealed by Raman Scattering and Optical Ellipsometry

Yuan Li,^{1,2,*} M. Le Tacon,^{2,†} Y. Matiks,² A. V. Boris,² T. Loew,² C. T. Lin,² Lu Chen,¹ M. K. Chan,³ C. Dorow,³ L. Ji,³ N. Barišić,^{3,4} X. Zhao,^{3,5} M. Greven,³ and B. Keimer²

¹International Center for Quantum Materials, School of Physics, Peking University, Beijing 100871, China

²Max Planck Institute for Solid State Research, D-70569 Stuttgart, Germany

³School of Physics and Astronomy, University of Minnesota, Minneapolis, Minnesota 55455, USA

⁴Service de Physique de l'Etat Condensé, CEA-DSM-IRAMIS, F-91198 Gif-sur-Yvette, France

⁵State Key Lab of Inorganic Synthesis and Preparative Chemistry, College of Chemistry,

Jilin University, Changchun 130012, People's Republic of China

(Received 19 June 2013; published 30 October 2013)

We study the model high-temperature superconductor $\text{HgBa}_2\text{CuO}_{4+\delta}$ with electronic Raman scattering and optical ellipsometry over a wide doping range. The dependence of the resonant Raman cross section on the incident photon energy changes drastically as a function of doping, in a manner that corresponds to a rearrangement of the interband optical transitions seen with ellipsometry. This doping-dependent Raman resonance allows us to reconcile the apparent discrepancy between Raman and x-ray detection of magnetic fluctuations in superconducting cuprates. Intriguingly, the strongest variation occurs across the doping level where the antinodal superconducting gap appears to reach its maximum.

DOI: [10.1103/PhysRevLett.111.187001](https://doi.org/10.1103/PhysRevLett.111.187001)

PACS numbers: 74.25.nd, 74.40.-n, 74.72.Gh, 74.72.Kf

Magnetic fluctuations might play an essential role in the mechanism of high-temperature superconductivity in the cuprates [1]. In the antiferromagnetic (AFM) parent compounds, the spin fluctuations are magnons with energies up to ~ 300 meV. Since this energy is in principle sufficient to support superconductivity at very high temperatures, the observation of similar “paramagnon” excitations by resonant inelastic x-ray scattering (RIXS) in superconducting cuprates [2] is a revealing result. Recent electronic Raman scattering (ERS) measurements further suggest that the high-energy magnetic fluctuations are profoundly affected by the formation of Cooper pairs [3], corroborating a close connection between them.

Here we address a major puzzle that has arisen from the comparison of the doping dependent RIXS and ERS cross sections. Both techniques use inelastic photon scattering to probe fundamental excitations in solids, but with very different incident photon energies, and they can detect magnetic fluctuations in the cuprates via the creation of single- [4] and two-magnon [5] excitations, respectively. In the parent compounds, the superexchange energies J determined by RIXS and ERS agree reasonably well [4,5] and are consistent with inelastic neutron scattering (INS) results [6]. A comparison between these measurements at nonzero doping, however, reveals an important discrepancy: while the energy and spectral weight of the (para) magnon excitations observed by RIXS exhibit little change with doping [2,7], both of these quantities decrease substantially in ERS data [8–12]. The latter observation has created the impression that the AFM spin fluctuations become overdamped near and above optimal doping [9].

This, in turn, has served as a major argument against magnetically driven Cooper pairing in the overdoped regime [13,14]. Together with the gradual fade-out of the high-energy magnetic signal with doping in INS measurements [15], this has cast doubt on the interpretation of the RIXS results [16,17].

The RIXS cross section in the cuprates is known to exhibit a nontrivial photon energy dependence [18,19]. Detection of magnetic excitations is greatly enhanced by a resonant process that involves an intermediate state with strong spin-orbit coupling [17,20]. Similarly, the ERS detection of two-magnon excitations is assisted by resonant Raman processes [21,22]. For undoped systems, a strong enhancement of the signal is found for incident photon energies in the 2.4–3.0 eV range [8,9,13,23], and it has been common practice to use fixed laser energies suitable for the study of the undoped systems to perform measurements at nonzero doping [10–12]. A caveat is that the doping dependence of the ERS signal measured in this fashion may reflect variations not only in the magnetic excitations, but also in the resonant process [8].

We have determined the origin of the discrepancy between the RIXS and ERS results by performing ERS measurements in the model high-temperature superconductor $\text{HgBa}_2\text{CuO}_{4+\delta}$ (Hg1201). We used two distinct incident photon energies for our ERS measurements and performed complementary ellipsometry measurements on the same samples, in order to monitor any possible change in the Raman resonance. At low doping, the ERS two-magnon signal is resonantly enhanced at the higher incident photon energy, but as the hole concentration is

increased beyond $p \approx 0.10$, the resonant condition changes and favors the lower incident photon energy. The change coincides with a rearrangement of interband transitions in the 1–3 eV range observed by ellipsometry. Our observation of strong two-magnon signals at doping levels as high as $p = 0.19$, albeit only under a resonant condition that is different from that for undoped and lightly doped cuprates, demonstrates that the amplitude of the ERS signal is predominantly affected by the resonant process, and that short-range high-energy AFM fluctuations do exist up to rather high doping. Furthermore, we find that the ERS B_{1g} gap in the superconducting state reaches its maximum near the same doping level where the crossover between different resonant conditions occurs.

Our measurements were performed on eight single crystals of Hg1201 grown by a self-flux method [24] and postgrowth annealed to control the doping level [25]. The samples are denoted by UD (underdoped) or OV (overdoped) followed by their critical temperature (T_c) values in Kelvin. Nominal hole concentrations are calculated from T_c according to an empirical formula [26]. The ERS measurements were performed using a Jobin Yvon LabRam spectrometer in a quasibackscattering geometry on freshly polished surfaces parallel to the ab plane. The ellipsometry measurements were performed using a Woollam VASE spectrometer. Further details can be found in the Supplemental Material [27].

Figure 1 displays Raman B_{1g} spectra for a heavily (UD45) and a slightly underdoped (UD94) Hg1201 sample, along with data measured on an AFM insulating $\text{YBa}_2\text{Cu}_3\text{O}_{6.1}$ (YBCO_{6.1}) sample. Spectra measured on a silicon (100) surface, which gives no ERS or fluorescence signal in the displayed range (Fig. S1 in the Supplemental Material [27]), are shown for comparison, and we only consider features that are absent from the Si spectra as genuine ERS signals. In YBCO_{6.1}, the two-magnon peak is observed at about 320 meV with 2.33 eV incident photons, but not clearly with 1.96 eV incident photons. In the latter “off-resonance” condition, the ERS signal shows a depletion at low temperature below 320 meV, identical to the peak position seen with the “on-resonance” condition. This correspondence is utilized later. The Hg1201 UD45 sample looks qualitatively similar to YBCO_{6.1}. However, a very different behavior is found for UD94: the two-magnon peak can be observed with 1.96 eV incident photons already at $T = 300$ K and its amplitude is larger at $T = 10$ K [3], but no clear peak can be observed with 2.33 eV incident photons. This is best contrasted by comparing the data for UD45 and UD94 obtained with the same photon energy. This observation indicates a doping dependence of the Raman resonant condition, with different required incident photon energies at low and high doping.

Figure 2(a) shows this systematically by displaying the difference between B_{1g} spectra taken at 10 and 300 K for all our samples with 1.96 eV incident photons. A crossover

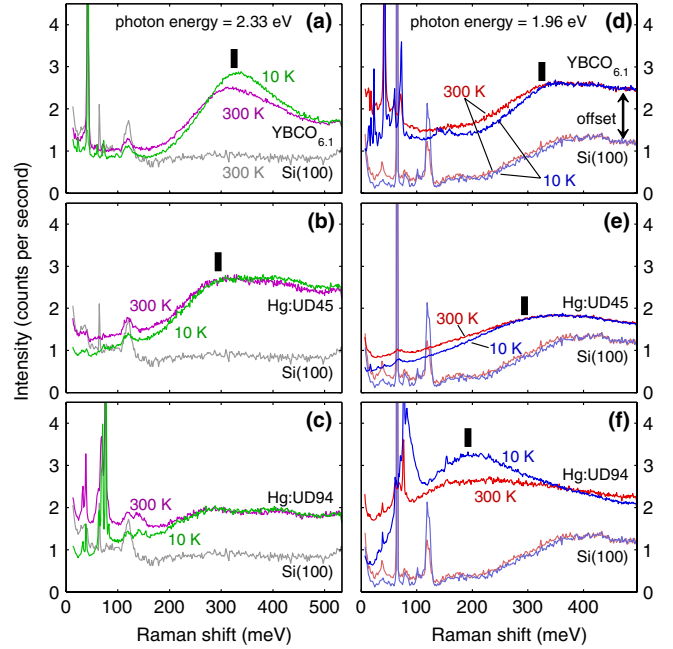


FIG. 1 (color online). Raw Raman spectra for $\text{YBa}_2\text{Cu}_3\text{O}_{6.1}$ (a), (d), Hg1201 UD45 (b),(e), and UD94 (c),(f) obtained with 2.33 (a)–(c) and 1.96 eV (d)–(f) incident photons in the B_{1g} scattering geometry. Data obtained on Si(100) surface are displayed for comparison (see text). The small feature in (b),(c) at ~ 410 meV is due to fluorescence and/or an experiment artifact.

from depletion to enhancement at low temperature is found as the doping level is increased beyond that of the UD64 sample. A pronounced two-magnon signal appears in the raw data above the same doping level (Fig. S2 in the

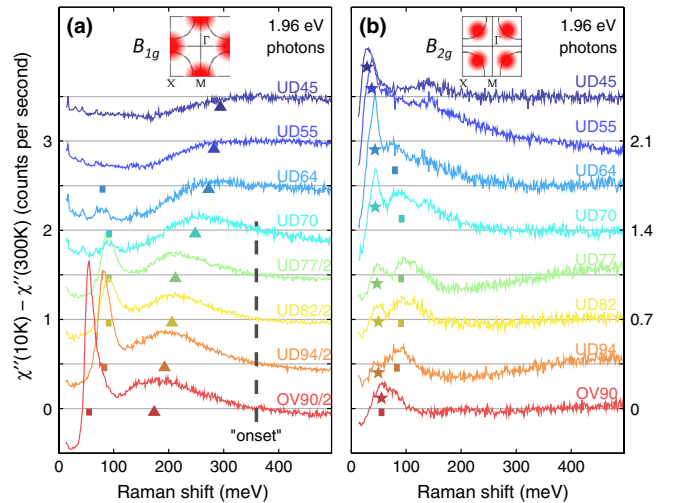


FIG. 2 (color online). Difference between Raman susceptibility at 10 and 300 K measured with 1.96 eV incident photons in the B_{1g} (a) and B_{2g} (b) geometries, offset for clarity. Symbols indicate characteristic energies (see text). The bottom four spectra in (a) have been divided by a factor of 2 to allow a common scale.

Supplemental Material [27]). The absence of similar effects in A_{1g} (Fig. S3 in the Supplemental Material [27]) and B_{2g} data [Fig. 2(b)] shows that the signal exclusively belongs to the B_{1g} irreducible representation of the D_{4h} group, consistent with our interpretation of it as two-magnon excitations evolving from the undoped AFM insulator. The prominent signal at high doping highlights the main finding of our work: When measured with a photon energy that satisfies the resonant condition at high (but not at low) doping, the two-magnon intensity exhibits an unexpected doping dependence. The discrepancy between the ERS and RIXS results concerning the magnon intensity can hence be explained by the (hitherto undetected) doping-dependent Raman resonance. Indeed, both the ERS and RIXS magnon cross sections are greatly enhanced by photon scattering resonances; but unlike the latter, which involves (doping-independent) Cu $2p$ core holes as intermediate states, the former is related to interband transitions in the visible range and is strongly dependent on doping. The data in Fig. 2(a) indicate that short-range high-energy AFM fluctuations are present up to at least $p = 0.19$.

Another issue in the comparison between ERS and RIXS concerns the magnon energy. In Fig. 2(a), the energy (triangles) determined from the position of either the depletion at low doping or the maximal enhancement at high doping (which are treated on equal footing as suggested by the on- and off-resonance correspondence in Fig. 1), decreases with doping [10–12]. However, because this energy might be affected by the doping-dependent resonant process and/or the size of the pseudogap, and especially by magnon-magnon interactions [17], it might not correspond to any observable feature in the single-magnon spectrum measured with RIXS. We notice that the highest energy of the enhancement [dashed line in Fig. 2(a)] is almost doping independent. This energy might be related to the hole doping-independent magnon energy observed by RIXS [2,7].

The spectra in Fig. 2 contain low-energy ERS signals associated with superconductivity. They are marked by rectangles and asterisks for the B_{1g} and B_{2g} geometries, which selectively probe electronic transitions in the antinodal and nodal regions of the Brillouin zone [22], respectively. The data are in good overall agreement with reported ERS results for Hg1201 and other cuprates: the B_{1g} energy decreases as optimal doping is approached from below while the B_{2g} energy increases [28–30], and the intensity of the B_{1g} peak increases rapidly with overdoping [30]. Here we focus on the underdoped side and report a few observations.

(i) The decrease and eventual disappearance of the B_{1g} peak with underdoping resembles the behavior of the two-magnon peak. This suggests that the two features are enhanced by similar resonant effects.

(ii) The B_{1g} energy is also visible in the B_{2g} data as indicated by rectangular symbols in Fig. 2(b). While we do

not know the exact reason for this, we can rule out polarization leakage which we estimate to be less than 3% based on phonon intensities observed in the different geometries. Our data do not contradict previous reports [28–31], where the use of different incident photon energies and/or a smaller separation between the B_{1g} and B_{2g} energies might have prevented a similar observation. At low doping, the B_{2g} signal exhibits a long tail extending above 120 meV. This component of the signal persists above T_c (not shown) and might be a signature of a pseudogap recently proposed to have an s -wave form [32]. The B_{2g} double-peak structure resembles a recent theoretical proposal of Higgs-boson-like excitations [33].

(iii) We observe the B_{1g} peak down to an unprecedentedly low doping level of $p \approx 0.09$ (UD64), and see a clear decrease of its energy below $p \approx 0.10$ (Fig. S4 in the Supplemental Material [27]). A similar decrease of the d -wave superconducting gap has been observed by photoemission for Bi2212 below $p \approx 0.08$ [34].

We summarize our ERS results in Fig. 3. The dashed line indicates where the rearrangement of optical interband transitions occurs (see below). The two-magnon signal seen with 1.96 eV incident photons changes its temperature dependence from depletion (empty triangles) to enhancement (filled triangles) at low temperature upon crossing this line, and its energy exhibits a sudden decrease. Intriguingly, the B_{1g} superconducting gap reaches its maximum near the same doping.

The Raman resonance is linked to absorption and/or emission of photons of specific energies [21,22], and is expected to be sensitive to specific features in the optical properties of the material. We therefore performed ellipsometry measurements on the same samples to further verify the conclusion of our ERS study. Ellipsometry has the advantage of measuring both the real and imaginary parts of the optical constants, leaving the Kramers-Kronig relations as a strong constraint on data fitting.

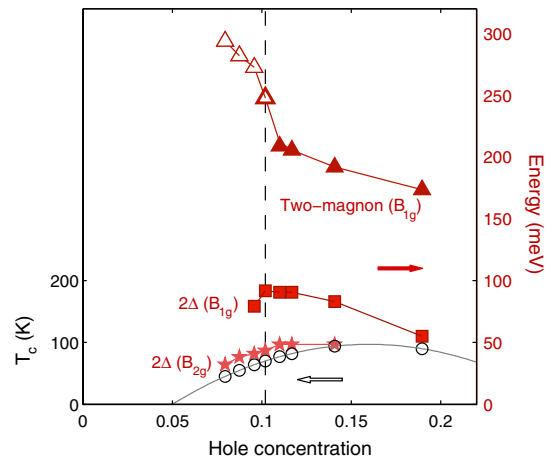


FIG. 3 (color online). Summary of ERS characteristic energies. Same symbols are used as in Fig. 2.

Figure 4(a) displays the imaginary part of the dielectric function at 300 K. In addition to a Drude response, the evolution with doping in the 0.8–3.2 eV range can be described by four Lorentzian oscillators modeling interband transitions, as labeled in the inset, where data obtained at 10 K show that the spectrum is nearly temperature independent apart from thermal broadening (Fig. S5 of the Supplemental Material [27]). The α and δ transitions are slightly below and above our ERS incident photon energies, so they are favorable for 1.96 and 2.33 eV incident photons, respectively [Fig. 4(b)]. Because β is close to both our incident photon energies, and γ does not exhibit systematic doping dependence, they are not expected to clearly enhance the Raman cross section for either of the incident photon energies. The oscillator strengths of these transitions are obtained by simultaneously fitting the real and imaginary parts (Fig. S6 in the Supplemental Material [27]) and summarized in Fig. 4(c). Indeed, we find that the δ and α transitions are prominent at low and high doping, respectively, with a crossover near UD70 ($p \approx 0.10$). This precisely corresponds to our observation of prominent ERS two-magnon signals with 2.33 and 1.96 eV incident photons at low and high doping, respectively. It confirms our interpretation of the results in Figs. 1 and 2(a) in terms of a doping-dependent Raman resonance.

Our result sheds light on the nature of the relevant high-energy electronic states. At low doping, the Raman resonance has been the subject of considerable theoretical investigations [21,35], and it generally requires the

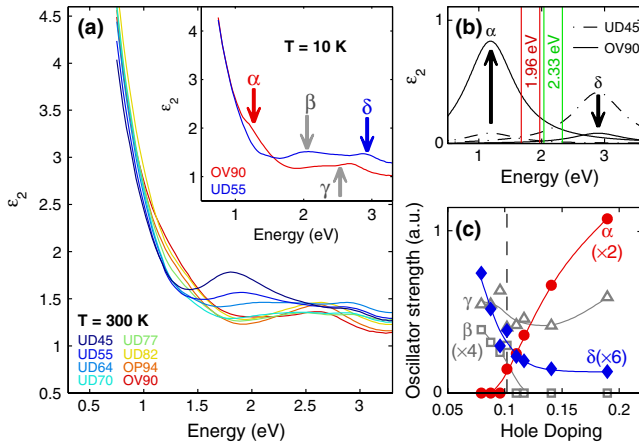


FIG. 4 (color online). (a) Imaginary part of dielectric constant measured at 300 K. Inset: measurements at 10 K, where individual transitions are better seen (Fig. S5 in the Supplemental Material [27] shows the full temperature dependence). (b) Schematic of the α and δ transitions relative to our ERS photon energies. The two vertical lines for each incident-photon wavelength indicate the energies of the incident and scattered photons (after creating the two-magnon excitations). (c) Fit oscillator strength of the transitions labeled in (a) at 300 K. Other fit parameters are presented in Fig. S7 and Table I in the Supplemental Material [27].

absorption of photons that are energetic enough to overcome the effective Hubbard repulsion, which is the charge-transfer gap. According to Fig. 4(a), however, the α transition does not evolve continuously out of any of the other transitions: β is the only transition nearby but its energy increases with doping. Most likely, the α transition involves a new band that develops at high doping, inside the charge-transfer gap which is present in Hg1201 up to at least optimal doping [18], suggesting that a rigid-band picture is insufficient for the description of the doping evolution of high-energy electronic states.

Similar developments of new interband transitions in the 0.8–1.5 eV range at high doping have been found in YBCO (Ref. [8]), $\text{La}_{2-x}\text{Sr}_x\text{CuO}_4$ (Ref. [36]), and $\text{Bi}_2\text{Sr}_2\text{Ca}_{0.92}\text{Y}_{0.08}\text{Cu}_2\text{O}_{8+\delta}$ (Ref. [37]), but they have not been associated with any Raman resonance prior to our work. The counterpart of α in $\text{La}_{2-x}\text{Sr}_x\text{CuO}_4$ has been attributed to a transition from a localized polaronic state inside the charge-transfer gap to an extended state above the gap [38]. Other possibilities, such as a breakdown of the Zhang-Rice singlet approximation at high doping [39], doped holes not entering the planar orbitals [40], or splitting of the charge-transfer peak with the suppression of AFM correlations [41], cannot be ruled out at this time. Band-structure calculations for undoped Hg1201 indicate the presence of a Hg-O band not far from the Fermi level which may evolve with doping [42], but this scenario would have difficulty explaining the Raman resonance, because the spatial separation between the Cu-O and Hg layers is large. First-principles calculations for doped Hg1201 are challenging due to the complex dopant oxygen positions, which have not yet been fully determined [43].

To conclude, we have identified a pronounced doping dependence of the Raman resonance in Hg1201, both by direct observation of the two-magnon ERS signal at high doping under nonstandard conditions, and by the observation of a rearrangement of interband transitions near $p = 0.10$ via ellipsometry. Our data show the presence of short-range high-energy AFM fluctuations in the overdoped regime, and they allow us to reconcile the discrepancy between existing ERS and RIXS results. Further research is needed to understand the exact nature of the high-energy electronic states involved in the Raman resonance, which appear to affect the size of the superconducting gap.

We wish to thank P. Bourges, A. Chubukov, M. Civelli, T. Devereaux, R. Hackl, T. Tohyama, C. M. Varma, Z.-Y. Weng, and A. Yaresko for stimulating discussions and Armin Schultz for technical assistance. Y.L. acknowledges the Alexander von Humboldt foundation and start-up support from Peking University. Crystal growth and characterization work at the University of Minnesota are supported by the Department of Energy, Office of Basic Energy Sciences, under Award No. DE-SC0006858.

- *yuan.li@pku.edu.cn
†m.letacon@fkf.mpg.de
- [1] D. J. Scalapino, *Phys. Rep.* **250**, 329 (1995); A. Abanov, A. V. Chubukov, and J. Schmalian, *Adv. Phys.* **52**, 119 (2003); T. Moriya and K. Ueda, *Rep. Prog. Phys.* **66**, 1299 (2003).
 - [2] M. Le Tacon, G. Ghiringhelli, J. Chaloupka, M. Moretti Sala, V. Hinkov, M. W. Haverkort, M. Minola, M. Bakr, K. J. Zhou, S. Blanco-Canosa, C. Monney, Y. T. Song, G. L. Sun, C. T. Lin, G. M. De Luca, M. Salluzzo, G. Khaliullin, T. Schmitt, L. Braicovich, and B. Keimer, *Nat. Phys.* **7**, 725 (2011).
 - [3] Y. Li, M. Le Tacon, M. Bakr, D. Terrade, D. Manske, R. Hackl, L. Ji, M. K. Chan, N. Barišić, X. Zhao, M. Greven, and B. Keimer, *Phys. Rev. Lett.* **108**, 227003 (2012).
 - [4] L. Braicovich, J. van den Brink, V. Bisogni, M. Moretti Sala, L. J. P. Ament, N. B. Brookes, G. M. De Luca, M. Salluzzo, T. Schmitt, V. N. Strocov, and G. Ghiringhelli, *Phys. Rev. Lett.* **104**, 077002 (2010).
 - [5] K. B. Lyons, P. A. Fleury, J. P. Remeika, A. S. Cooper, and T. J. Negran, *Phys. Rev. B* **37**, 2353 (1988).
 - [6] R. Coldea, S. M. Hayden, G. Aeppli, T. G. Perring, C. D. Frost, T. E. Mason, S.-W. Cheong, and Z. Fisk, *Phys. Rev. Lett.* **86**, 5377 (2001).
 - [7] M. Le Tacon, M. Minola, D. C. Peets, M. Moretti Sala, S. Blanco-Canosa, V. Hinkov, R. Liang, D. A. Bonn, W. N. Hardy, C. T. Lin, T. Schmitt, L. Braicovich, G. Ghiringhelli, and B. Keimer, *Phys. Rev. B* **88**, 020501 (2013); M. P. M. Dean, G. Dellea, R. S. Springell, F. Yakhov-Harris, K. Kummer, N. B. Brookes, X. Liu, Y.-J. Sun, J. Strle, T. Schmitt, L. Braicovich, G. Ghiringhelli, I. Božović, and J. P. Hill, *Nat. Mater.* (to be published).
 - [8] S. L. Cooper, D. Reznik, A. Kotz, M. A. Karlow, R. Liu, M. V. Klein, W. C. Lee, J. Giapintzakis, D. M. Ginsberg, B. W. Veal, and A. P. Paulikas, *Phys. Rev. B* **47**, 8233 (1993).
 - [9] G. Blumberg, R. Liu, M. V. Klein, W. C. Lee, D. M. Ginsberg, C. Gu, B. W. Veal, and B. Dabrowski, *Phys. Rev. B* **49**, 13295 (1994).
 - [10] M. Rübhausen, C. T. Rieck, N. Dieckmann, K.-O. Subke, A. Bock, and U. Merkt, *Phys. Rev. B* **56**, 14797 (1997).
 - [11] S. Sugai, H. Suzuki, Y. Takayanagi, T. Hosokawa, and N. Hayamizu, *Phys. Rev. B* **68**, 184504 (2003).
 - [12] B. Muschler, W. Prestel, L. Tassini, R. Hackl, M. Lambacher, A. Erb, S. Komiyama, Y. Ando, D. Peets, W. Hardy, R. Liang, and D. Bonn, *Eur. Phys. J. Special Topics* **188**, 131 (2010); L. Tassini, W. Prestel, A. Erb, M. Lambacher, and R. Hackl, *Phys. Rev. B* **78**, 020511 (2008).
 - [13] M. Rübhausen, O. A. Hammerstein, A. Bock, U. Merkt, C. T. Rieck, P. Guptasarma, D. G. Hinks, and M. V. Klein, *Phys. Rev. Lett.* **82**, 5349 (1999).
 - [14] E. G. Maksimov, M. L. Kulić, and O. V. Dolgov, *Adv. Condens. Matter Phys.* **2010**, 423725 (2010).
 - [15] S. Wakimoto, K. Yamada, J. M. Tranquada, C. D. Frost, R. J. Birgeneau, and H. Zhang, *Phys. Rev. Lett.* **98**, 247003 (2007); O. J. Lipscombe, S. M. Hayden, B. Vignolle, D. F. McMorrow, and T. G. Perring, *Phys. Rev. Lett.* **99**, 067002 (2007); C. Stock, R. A. Cowley, W. J. L. Buyers, C. D. Frost, J. W. Taylor, D. Peets, R. Liang, D. Bonn, and W. N. Hardy, *Phys. Rev. B* **82**, 174505 (2010).
 - [16] J. M. Tranquada, G. Xu, and I. A. Zaliznyak, *arXiv:1301.5888* [J. Magn. Magn. Mater. (to be published)].
 - [17] C. J. Jia, E. A. Nowadnick, K. Wohlfeld, C.-C. Chen, S. Johnston, T. Tohyama, B. Moritz, and T. P. Devereaux, *arXiv:1308.3717*.
 - [18] L. Lu, G. Chabot-Couture, X. Zhao, J. N. Hancock, N. Kaneko, O. P. Vajk, G. Yu, S. Grenier, Y. J. Kim, D. Casa, T. Gog, and M. Greven, *Phys. Rev. Lett.* **95**, 217003 (2005).
 - [19] L. Lu, J. N. Hancock, G. Chabot-Couture, K. Ishii, O. P. Vajk, G. Yu, J. Mizuki, D. Casa, T. Gog, and M. Greven, *Phys. Rev. B* **74**, 224509 (2006).
 - [20] L. J. P. Ament, G. Ghiringhelli, M. M. Sala, L. Braicovich, and J. van den Brink, *Phys. Rev. Lett.* **103**, 117003 (2009); M. W. Haverkort, *Phys. Rev. Lett.* **105**, 167404 (2010).
 - [21] B. S. Shastry and B. I. Shraiman, *Int. J. Mod. Phys. B* **05**, 365 (1991).
 - [22] T. P. Devereaux and R. Hackl, *Rev. Mod. Phys.* **79**, 175 (2007).
 - [23] M. Yoshida, S. Tajima, N. Koshizuka, S. Tanaka, S. Uchida, and T. Itoh, *Phys. Rev. B* **46**, 6505 (1992).
 - [24] X. Zhao, G. Yu, Y.-C. Cho, G. Chabot-Couture, N. Barišić, P. Bourges, N. Kaneko, Y. Li, L. Lu, E. M. Motoyama, O. P. Vajk, and M. Greven, *Adv. Mater.* **18**, 3243 (2006).
 - [25] N. Barišić, Y. Li, X. Zhao, Y.-C. Cho, G. Chabot-Couture, G. Yu, and M. Greven, *Phys. Rev. B* **78**, 054518 (2008).
 - [26] J. L. Tallon, C. Bernhard, H. Shaked, R. L. Hitterman, and J. D. Jorgensen, *Phys. Rev. B* **51**, 12911 (1995).
 - [27] See Supplemental Material at <http://link.aps.org/supplemental/10.1103/PhysRevLett.111.187001> for supporting data and details of our methods and analyses.
 - [28] M. Le Tacon, A. Sacuto, A. Georges, G. Kotliar, Y. Gallais, D. Colson, and A. Forget, *Nat. Phys.* **2**, 537 (2006).
 - [29] S. Blanc, Y. Gallais, M. Cazayous, M. A. Méasson, A. Sacuto, A. Georges, J. S. Wen, Z. J. Xu, G. D. Gu, and D. Colson, *Phys. Rev. B* **82**, 144516 (2010).
 - [30] N. Munnikes, B. Muschler, F. Venturini, L. Tassini, W. Prestel, S. Ono, Y. Ando, D. C. Peets, W. N. Hardy, R. Liang, D. A. Bonn, A. Damascelli, H. Eisaki, M. Greven, A. Erb, and R. Hackl, *Phys. Rev. B* **84**, 144523 (2011).
 - [31] Y. Gallais, A. Sacuto, T. P. Devereaux, and D. Colson, *Phys. Rev. B* **71**, 012506 (2005).
 - [32] S. Sakai, S. Blanc, M. Civelli, Y. Gallais, M. Cazayous, M.-A. Méasson, J. S. Wen, Z. J. Xu, G. D. Gu, G. Sangiovanni, Y. Motome, K. Held, A. Sacuto, A. Georges, and M. Imada, *Phys. Rev. Lett.* **111**, 107001 (2013).
 - [33] Y. Barlas and C. M. Varma, *Phys. Rev. B* **87**, 054503 (2013).
 - [34] K. Tanaka, W. S. Lee, D. H. Lu, A. Fujimori, T. Fujii, Risdiana, I. Terasaki, D. J. Scalapino, T. P. Devereaux, Z. Hussain, and Z.-X. Shen, *Science* **314**, 1910 (2006); I. M. Vishik, M. Hashimoto, R.-H. He, W.-S. Lee, F. Schmitt, D. Lu, R. G. Moore, C. Zhang, W. Meevasana, T. Sasagawa, S. Uchida, K. Fujita, S. Ishida, M. Ishikado, Y. Yoshida, H. Eisaki, Z. Hussain, T. P. Devereaux, and Z.-X. Shen, *Proc. Natl. Acad. Sci. U.S.A.* **109**, 18332 (2012).

- [35] A. V. Chubukov and D. M. Frenkel, *Phys. Rev. Lett.* **74**, 3057 (1995); *Phys. Rev. B* **52**, 9760 (1995); E. Hanamura, N. T. Dan, and Y. Tanabe, *Phys. Rev. B* **62**, 7033 (2000); T. Tohyama, H. Onodera, K. Tsutsui, and S. Maekawa, *Phys. Rev. Lett.* **89**, 257405 (2002); I. Kupčić, *J. Raman Spectrosc.* **42**, 998 (2011).
- [36] S. Uchida, T. Ido, H. Takagi, T. Arima, Y. Tokura, and S. Tajima, *Phys. Rev. B* **43**, 7942 (1991).
- [37] C. Giannetti, F. Cilento, S. Dal Conte, G. Coslovich, G. Ferrini, H. Molegraaf, M. Raichle, R. Liang, H. Eisaki, M. Greven, A. Damascelli, D. van der Marel, and F. Parmigiani, *Nat. Commun.* **2**, 353 (2011).
- [38] J. Lorenzana and L. Yu, *Phys. Rev. Lett.* **70**, 861 (1993).
- [39] M. Schneider, R.-S. Unger, R. Mitdank, R. Müller, A. Krapf, S. Rogaschewski, H. Dwelk, C. Janowitz, and R. Manzke, *Phys. Rev. B* **72**, 014504 (2005); D. C. Peets, D. G. Hawthorn, K. M. Shen, Y.-J. Kim, D. S. Ellis, H. Zhang, S. Komiya, Y. Ando, G. A. Sawatzky, R. Liang, D. A. Bonn, and W. N. Hardy, *Phys. Rev. Lett.* **103**, 087402 (2009).
- [40] C. T. Chen, L. H. Tjeng, J. Kwo, H. L. Kao, P. Rudolf, F. Sette, and R. M. Fleming, *Phys. Rev. Lett.* **68**, 2543 (1992); M. Merz, N. Nücker, P. Schweiss, S. Schuppler, C. T. Chen, V. Chakarian, J. Freeland, Y. U. Idzerda, M. Kläser, G. Müller-Vogt, and T. Wolf, *Phys. Rev. Lett.* **80**, 5192 (1998).
- [41] T. A. Sedrakyan and A. V. Chubukov, *Phys. Rev. B* **81**, 174536 (2010).
- [42] H. Sakakibara, H. Usui, K. Kuroki, R. Arita, and H. Aoki, *Phys. Rev. B* **85**, 064501 (2012); T. Das, *Phys. Rev. B* **86**, 054518 (2012).
- [43] M. Izquierdo, S. Megtert, D. Colson, V. Honkimäki, A. Forget, H. Raffy, and R. Comès, *J. Phys. Chem. Solids* **72**, 545 (2011); G. Chabot-Couture, Ph.D thesis, Stanford University, 2010.